Computer Methods and Programs in Biomedicine 195 (2020) 105558

Contents lists available at ScienceDirect

Computer Methods and Programs in Biomedicine

journal homepage: www.elsevier.com/locate/cmpb

Wavelet denoising as a post-processing enhancement method for non-invasive foetal electrocardiography

Giulia Baldazzi[a,b,1,*], Eleonora Sulas[a,1], Monica Urru[c], Roberto Tumbarello[c], Luigi Raffo[a], Danilo Pani[a]

[a] DIEE, Department of Electrical and Electronic Engineering, University of Cagliari, Piazza d'Armi, 09122 Cagliari, Italy
[b] DIBRIS, Department of Informatics, Bioengineering, Robotics and Systems Engineering, University of Genoa, Via Opera Pia 13, 16145 Genoa, Italy
[c] Division of Paediatric Cardiology, San Michele Hospital, Piazzale Alessandro Ricchi 1, 09134 Cagliari, Italy

ARTICLE INFO

Article history:
Received 21 January 2020
Revised 30 April 2020
Accepted 18 May 2020

Keywords:
Non-invasive foetal ECG
Wavelet denoising
Post-processing
Stationary wavelet transform
Wavelet packet

ABSTRACT

Background and Objective: The detection of a clean and undistorted foetal electrocardiogram (fECG) from non-invasive abdominal recordings is an open research issue. Several physiological and instrumental noise sources hamper this process, even after that powerful fECG extraction algorithms have been used. Wavelet denoising is widely used for the improvement of the SNR in biomedical signal processing. This work aims to systematically assess conventional and unconventional wavelet denoising approaches for the post-processing of fECG signals by providing evidence of their effectiveness in improving fECG SNR while preserving the morphology of the signal of interest.

Methods: The stationary wavelet transform (SWT) and the stationary wavelet packet transform (SWPT) were considered, due to their different granularity in the sub-band decomposition of the signal. Three thresholds from the literature, either conventional (Minimax and Universal) and unconventional, were selected. To this aim, the unconventional one was adapted for the first time to SWPT by trying different approaches. The decomposition depth was studied in relation to the characteristics of the fECG signal. Synthetic and real datasets, publicly available for benchmarking and research, were used for quantitative analysis in terms of noise reduction, foetal QRS detection performance and preservation of fECG morphology.

Results: The adoption of wavelet denoising approaches generally improved the SNR. Interestingly, the SWT methods outperformed the SWPT ones in morphology preservation ($p<0.04$) and SNR ($p<0.0003$), despite their coarser granularity in the sub-band analysis. Remarkably, the Han *et al.* threshold, adopted for the first time for fECG processing, provided the best quality improvement ($p<0.003$).

Conclusions: The findings of our systematic analysis suggest that particular care must be taken when selecting and using wavelet denoising for non-invasive fECG signal post-processing. In particular, despite the general noise reduction capability, signal morphology can be significantly altered on the basis of the parameterization of the wavelet methods. Remarkably, the adoption of a finer sub-band decomposition provided by the wavelet packet was not able to improve the quality of the processing.

1. Introduction

Antenatal cardiac screening has relevant diagnostic value because of the relatively high incidence of congenital heart diseases, about 1% of live births [1]. In the diagnosis of such pathologies, the morphology of the cardiac electrical signal in early pregnancy would enrich the information provided by conventional ultrasonographic methods. Unfortunately, non-invasive foetal electrocardiography (fECG) is still far from being widely adopted [2] because of its complex setup and relatively low signal-to-noise ratio (SNR) [1]. The low SNR of non-invasive fECG is attributed to the instrumental noise, the maternal electrophysiological interferences and their spectral overlap with the signal of interest, the reduced size of the foetal heart and the attenuation of the signal due to the different

* Corresponding author.
E-mail address: giulia.baldazzi@unica.it (G. Baldazzi).
[1] These authors equally contributed.

https://doi.org/10.1016/j.cmpb.2020.105558

layers of tissue to be passed through for gathering the signal on the maternal skin. Moreover, starting from the 28th week of gestation, an electrically insulating layer, the *vernix caseosa*, considerably attenuates the non-invasive fECG up to about the 34th week, when the signal can be gathered again but with non-linear distortions [3].

Despite the number of techniques developed in the literature for fECG extraction, the identification of a clean and undistorted fECG signal remains an open research issue [4]. In this context, the wavelet transform (WT), a signal analysis tool widely used in biomedical signal processing, has been applied as a preprocessing tool [5] and for the fECG detection or extraction [6], alone [7–11] or along with other methods such independent component analysis [12,13] and adaptive filters [14–16]. Moreover, it was adopted in the form of wavelet denoising (WD) for the post-processing of the fECG, i.e. after a fECG extraction algorithm, for the improvement of the SNR, to achieve a better representation of the fECG signal morphology [17,18,27–31,19–26]. However, this technique has been generally applied simply to reduce noisy interferences after fECG extraction algorithms, but fundamental evidence about the different wavelet implementation choices and parameterizations was not deeply discussed nor the characteristics of the real or simulated data were always clearly stated. This fact hampers the identification of an effective wavelet methodology for fECG post-processing applications and the possibility to perform a comparative appraisal. Only in [31] and [5], an analysis of different WD algorithms and parameters was presented, albeit giving quantitative noise removal indications only on a limited set of simulated ECG signals affected by additive white gaussian noise in the former, while on a single fECG trace affected by muscular or powerline interference in the latter. Hence, to the best of authors' knowledge, a methodological study on the effect of WD on the post-processing of real and synthetic fECG signals is still missing.

This work aims to perform such an analysis, trying to answer relevant questions related to the optimal choices in terms of the granularity in the sub-band decomposition and of the thresholds able to combine an effective denoising with the preservation of the morphology of the fECG signal. To this aim, moving from our preliminary investigations on the topic [32], we explored the adoption of stationary wavelet transform (SWT) and stationary wavelet packet transform (SWPT), with different deepness of decomposition, chosen according to the fECG spectral characteristics. In order to assess the importance of the dependency between the scaling factors used in the threshold computation and the decomposition level, we also compared three thresholds taken from the scientific literature, either conventional [33,34] and unconventional [35]. For the latter, in this work we proposed and assessed for the first time some possible adaptations to the SWPT.

Results were systematically analysed by using different figures of merit, such as the SNR, the QRS complex detection accuracy and the true positive rate. The morphological distortions caused by WD were estimated by exploiting the root-mean-square error and the Spearman's and Pearson's correlation coefficients of the foetal beats. The analysis was performed on real and synthetic datasets of fECG signals extracted from non-invasive recordings. The adopted dataset is freely available for research purposes along with the accompanying Data in Brief article [36].

2. Materials and methods

WD is a signal processing technique based on the so-called time-scale representation, provided by the WT [37,38]. Among the different non-linear denoising techniques, WD is widely used in biomedical signal processing because of its good localization in the time and frequency domains. This feature is particularly useful when dealing with non-stationary signals, such as the biomedical ones [39,40]. Moreover, it allows noise removal when noisy interferences share the same spectral band of the signal of interest.

2.1. Background on WD

2.1.1. WT basic principles

The most widely used form of WT for fECG filtering is the discrete wavelet transform (DWT), which is characterised by a small distortion of QRS complex extremes [5]. It is based on the dyadic decomposition of the signal in sub-bands of different width [37]. It can be implemented by filter banks, including high-pass and low-pass filters whose definition is strictly associated with the chosen mother wavelet [37]. Such filters equally split in two the signal band: the outputs of this filtering step are known as *detail* and *approximation* at the first level and are associated with the higher and lower half-bands, respectively. Then, the same process is iteratively repeated on the output of the low-pass filter of the previous filtering step until the lowest frequency components, i.e. the approximation of the last level, cover the range between 0 and $f_n/2^l$, where f_n denotes the folding frequency and l the chosen decomposition level.

While only the approximation coefficients are given as input for the subsequent filtering steps in the WT, both detail and approximation are decomposed at each level in the wavelet packet decomposition [37], generating a complete decomposition binary tree with consequent sub-bands of the same width, equal to $f_n/2^l$. As such, a finer time-frequency analysis is obtained, as can be seen in Fig. 1.

2.1.2. WD basic principles

WD is essentially based on three main steps [37,40]. In the first one (*analysis*), the signal is decomposed in a set of wavelet coefficients by WT; then, detail coefficients are compared to a *threshold* (*thresholding* phase), and those that exceed the threshold are used along with the approximation for time-domain reconstruction (*synthesis*).

On the time-scale representation, the threshold is typically chosen to be proportional to the amount of noise, which, according to the noise affecting the signal of interest, can be estimated at each level as [33,34,37,41]:

$$\sigma_j = 1.4826 * median\left(\left|cD_j - \widehat{cD_j}\right|\right), \tag{1}$$

where cD_j represents the detail coefficients at the j-th level while $\widehat{cD_j}$ represents their median value. Aside from σ_j, the threshold is defined by a scaling factor that may be fixed or level-dependent. For instance, the Universal (2) and the Minimax (3) thresholds [33,34] are largely adopted.

$$\theta_j = \sigma_j \sqrt{2ln(N)}, \tag{2}$$

$$\theta_j = \sigma_j(0.3936 + 0.1829\log_2(N)). \tag{3}$$

Both thresholds depend on the signal length N. Once the threshold is computed at each detail level, different thresholding approaches can be implemented, but the most typical ones are the so-called *hard-thresholding* and *soft-thresholding* [33,34], which are respectively defined as:

$$\overline{cD_{j,k}} = \begin{cases} cD_{j,k} \; if \; \left|cD_{j,k}\right| \geq \theta_j \\ 0 \; otherwise \end{cases} \tag{4}$$

$$\overline{cD_{j,k}} = \begin{cases} sign(cD_{j,k})\left(\left|cD_{j,k}\right| - \theta_j\right) \; if \; \left|cD_{j,k}\right| \geq \theta_j \\ 0 \; otherwise \end{cases} \tag{5}$$

where $cD_{j,k}$ is the k-th detail coefficient at level j and θ_j is the threshold value calculated for the same level.

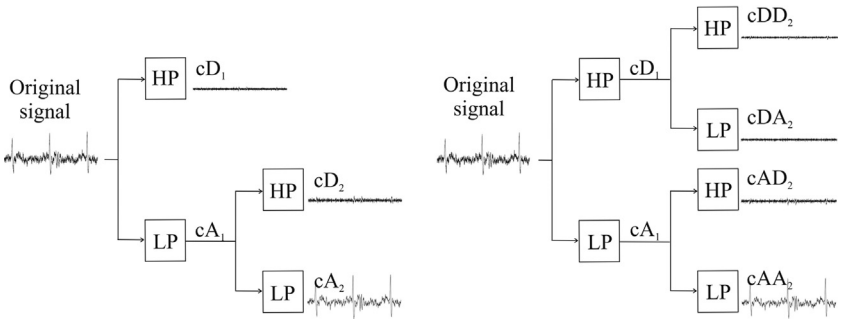

Fig. 1. Example of 2-level decomposition of a real fECG signal (@2048 Hz) with SWT (on the left) and SWPT (on the right).

2.2. WD algorithms and parameterizations studied

In WD algorithms, at each step, different implementation choices can influence the denoising result. In this work, some of these choices have been made basing on preliminary investigations, literature evidence or considerations associated with the specific problem of fECG denoising. They are reported at first in this section. Then, we will present the different options, compared and tested in this work, whose impact on the denoising process was unpredictable and worth to be analysed.

2.2.1. Basic parameterizations not assessed in this study

The choice of the mother wavelet affects the WD output. During a preliminary investigation with different mother wavelets, as confirmed by other studies [8], the Haar mother wavelet achieved better results. Thus, it was selected for this work, also taking into account its smallest support, the simplicity of the coefficients of its filters and the associated advantages in any real-time implementation.

In this work, we also selected hard-thresholding to avoid the shrinkage effect associated with soft-thresholding, which reduces the amplitude of the denoised signal and negatively affects the quality indexes that could be adopted for the performance assessment.

Finally, among the different implementations of the DWT, the SWT was chosen in this work because of its translation-invariance property [37,42–44]. For the same reasons described for the SWT, we used the SWPT [45,46] for the wavelet packet.

2.2.2. Advanced parameterizations assessed in this study

In this section, all the parameterizations and different algorithms compared in this work are presented, along with the motivations behind them.

As regards the decomposition level, we decided to test only two different parameterizations: six and seven levels, on the basis of the frequency contributions of major interest for foetal QRS complexes (8–20 Hz) [47] and the sampling frequency of the signals used in this work, which was equal to 2048 Hz. In 7-level decomposition, WD was performed from 1024 Hz down to 8 Hz (because details at level seven, cD_7, spread over the 8–16 Hz band); in 6-level decomposition, the lower limit for the details was 16 Hz (because the last detail, cD_6, spans over the 16–32 Hz band). As in every conventional WD algorithm, the approximation band was maintained without changes, so the low-frequency components associated with the other fECG waves are preserved by construction.

In WD, the selection of the threshold is particularly relevant since it determines the aggressivity of the denoising [5] and, therefore, the output SNR but also its morphological distortion. In this regard, we assumed the predominant presence of noise at high frequencies whereas a more significant signal content at low frequencies. For these reasons, we decided to test a threshold proposed by Han *et al.* in [35] for chaotic time series, defined in (6).

$$\theta_j = \begin{cases} \sigma_j\sqrt{2\ln(N)} & j = 1 \\ \sigma_j\sqrt{2\ln(N)/\ln(j+1)} & 1 < j < L \\ \sigma_j\sqrt{2\ln(N)}/\sqrt{j} & j = L \end{cases} \tag{6}$$

This unconventional threshold was conceived to perform a more aggressive denoising at higher frequencies while being more conservative at lower ones.

The Han *et al.* threshold was compared to other conventional thresholds whose adoption is widespread in ECG signal processing, i.e. the Universal (2) and the Minimax (3) [33,34].

Beyond the three thresholds and the two different levels of decomposition, a key aspect of this study was the assessment of SWT vs. SWPT. This is an interesting point, since the latter presents a finer granularity in the decomposition than the former, thus allowing more precise analysis of the signal, which is divided in equally-sized sub-bands. Despite its use in different application fields and the aforementioned potentialities, SWPT, and more generally the wavelet packet transform, is not used in fECG signal processing. To the best of our knowledge, a tentative approach was proposed only in [48] for powerline interference removal. To study its applicability to the fECG post-processing denoising, the adaptation of the Han *et al.* threshold was required, since this threshold was never used along with wavelet packet and it is funded on a level-dependent scaling factor of the estimated noise. Conversely, the transposition to the SWPT is direct for the Minimax and the Universal thresholds, by simply evaluating σ_j at each detail node. Three different adaptations of the Han *et al.* threshold, detailed in the following section, were compared in this work and the best performing one was adopted for the comparisons with the SWT.

2.2.3. Proposed adaptation of the Han et al. threshold to SWPT

The Han *et al.* threshold [35], originally conceived for DWT, uses a different scaling factor at the different levels (6), which in turn implies a bind between the scaling factor of the threshold and the spectral band of the details. It was then required to assign a scaling factor to each of the sub-bands of the SWPT decompositions. Three approaches were conceived, with a growing aggressiveness in terms of denoising. For all of them, we still evaluated σ_j at each detail node.

In the first approach, hereafter referred to as SWPT-LI, we exploited a simple linear interpolation of the scaling factor between the values defined for the SWT case. To be more conservative, we assigned the original threshold values to the highest leaf of each corresponding SWT detail sub-band and then computed the interpolated values for the remaining query points. This is the most conservative threshold.

In the second approach, hereafter referred to as SWPT-CI, we interpolated the missing threshold values with a piecewise cubic Hermite interpolating polynomial. Compared to the previous

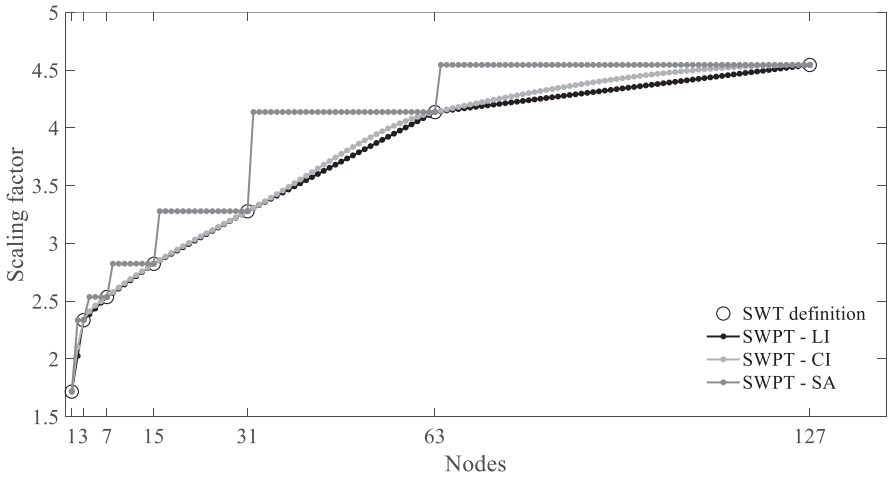

Fig. 2. Comparison of the different scaling factors proposed to adapt the Han *et al.* threshold to a 7-level decomposition with SWPT. Black circles report the values for the SWT definition. The three SWPT adaptations, namely the linear interpolation (SWPT-LI, in black), the cubic interpolation (SWPT-CI, in pale gray) and the spectral adaptation (SWPT-SA, in dark gray) are reported by putting in abscissa the SWPT nodes corresponding to specific spectral ranges: node 1 (8–16 Hz), node 3 (24–32 Hz), node 7 (56–64 Hz), node 15 (120–128 Hz), node 31 (248–256 Hz), node 63 (504–512 Hz) and node 127 (1016–1024 Hz).

approach, the shape-preserving characteristic of this interpolation method allowed achieving a smoothly changing scaling factor across the different nodes of the SWPT decomposition.

Finally, we evaluated the approach proposed in [32], hereafter referred to as SWPT-SA (for SWPT spectral adaptation). In this case, for each SWPT leaf, we adopted the same definition of the scaling factor as in (6) corresponding to the SWT detail level whose frequency band included that SWPT leaf. As can be seen in Fig. 2, this approach is the most aggressive one.

2.3. Testing datasets

Two datasets were created to perform the comparative assessment of the different WD methods. The first one was composed of physiologically-plausible synthetic fECG signals uncorrupted by the maternal interference whereas the second one was derived from real abdominal recordings after a fECG extraction processing based on an adaptive filtering. The two datasets allow studying different aspects of denoising. In fact, the signal distortion effect caused by WD can be evaluated only on the synthetic dataset, because a noise-free version of the fECG is available. However, such a dataset includes several ideal conditions that are not necessarily met at the output of a non-invasive fECG extraction method applied to real signals, motivating the adoption of a real dataset too.

Remarkably, the two datasets present only the fECG signal, i.e. the signal from the foetus “without” maternal interferences. For this reason, hereafter we will refer to fECG in this acceptation.

The synthetic dataset included 40 fECG signals, generated with an open-source non-invasive fECG signal simulator, FECGSYN [49–51], at 2048 Hz, with a duration of 10 s each. By construction, a single horizontal lead on the abdomen was obtained completely free of the maternal components. White and pink noises [52] were added to the traces, with amplitudes chosen according to the desired SNR (see Table 2, Figs. 2 and 3 in [36]).

For the computation of the WD threshold according to the different methods presented above, the noise level σ_j was evaluated on a part of the signal presenting only noise, i.e. approximately each interval between two foetal beats, since the mECG was not present.

The real dataset included 42 fECG signals, extracted from non-invasive recordings from 17 pregnant women with healthy foetuses between the 21st and 27th weeks of gestation (see Table 3 in [36]), sampled at 2048 Hz, with a duration of 15 s each. The exploration of different windows of the gestational age was beyond the scope of this work since it would mainly affect the SNR and the success rate in the fECG extraction process and not the post-processing. The fECG extraction algorithm was a multireference adaptive filter [53], given its numerical stability and good performance [54–56]. Adaptive filters are not able to reject noise sources not in common with the reference channels and, as such, they demand a post-processing denoising stage more than other techniques. For the same reason, all the leads were pre-processed with an high-pass filter with a cut-off frequency of 1 Hz, before fECG extraction, in order to facilitate the adaptive filter processing. Remarkably, the frequency range affected by this processing does not interfere with the assessment of the WD approaches but only with the fECG extraction process, since the removed frequencies would lie in the approximation band which is not affected by the denoising. A schematic representation of the electrodes placement was provided in [36], along with an illustrative figure of the processing stages and an example of the quality of the real signals (see Figs. 4–6 in [36]).

On the real dataset, the noise level σ_j in the different sub-bands was hampered by the possible presence of mECG residuals after the fECG extraction. In this case, a part of the signal representative only of the noise could be identified on the fECG leads between the time instants comprised between the end of a maternal T wave and the beginning of the maternal P wave of the next beat (delineated in a thoracic lead, where only the mECG is visible, by using the algorithm presented in [57]). This avoided considering maternal components in noise estimation. However, such signal segments were excluded in the presence of a foetal QRS complex in that interval.

For a complete description of the datasets, it is recommended to refer to the accompanying Data in Brief article [36], from which the signals can also be downloaded for research purposes.

2.4. Comparative analysis methods

The different parameterizations of the WD methods assessed in this work are summarised in Fig. 3. In the following paragraphs, we will describe at first the performance indexes used to perform the assessment and then the different comparisons between the WD methods along with the associated statistical analysis methodology.

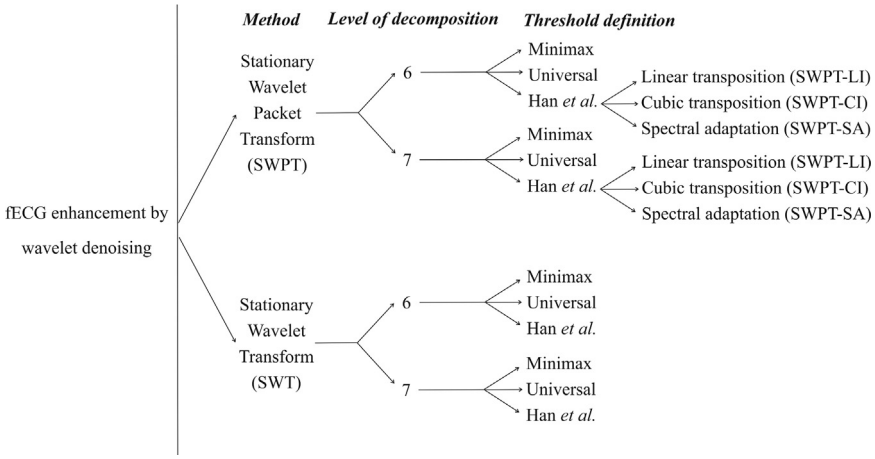

Fig. 3. All the wavelet parametrizations investigated in this work. Two translation-invariant wavelet transforms (SWT and SWPT) along with two different decomposition levels (six and seven) and three thresholds (Minimax, Universal, Han *et al.*) were assessed and compared. Specifically, due to its level-dependent scaling factor, three different SWPT transpositions were proposed and evaluated for the Han *et al.* threshold (SWPT-LI, SWPT-SA, SWPT-CI).

2.4.1. Performance indexes

The performance of the different WD approaches and parameterizations were systematically analysed by exploiting several indexes:

- SNR
- Foetal QRS detection accuracy (Acc)
- Foetal QRS detection true positive rate (TPR, or Sensitivity).

On the synthetic dataset, the following indexes were also evaluated:

- Root mean square error (RMSE)
- Pearson's correlation coefficient (ρ)
- Spearman's rank correlation coefficient (r_s).

The SNR is widely used to evaluate the quality of the trace in terms of power in the signal of interest and the noise sources. It was computed as:

$$SNR_{dB} = 20log_{10}\left(\frac{App_f}{4\sigma}\right) \quad (7)$$

where App_f is the peak-to-peak amplitude of the fECG and σ is the standard deviation of the noise. For the sake of the SNR calculation only, the estimation of the standard deviation of the noise was conceived as the median of the standard deviations computed on each interval between two foetal beats. This approach considers the presence of both the noise and potential residual mECG (the latter only in the real dataset).

Moreover, before the WD, we computed the App_f of a given signal on its average QRS complex, obtained by synchronized averaging, to reduce the inter-beat variability. On the simulated dataset, all foetal peaks were considered in the averaging since the signals were free from the mECG interference. In the real dataset, where mECG residuals could be present after the fECG extraction algorithm, the QRS averaging involved only those complexes exhibiting a Pearson's correlation coefficient above a given threshold, empirically chosen to be 0.6. If the number of correlated beats was lower than four, the signal was treated as non-deterministic, then substituting App_f by the computation of four times the median standard deviation of such beats.

To evaluate the SNR after the WD, we computed App_f as the median value of the peak-to-peak amplitudes of highly correlated beats or of all beats for real and simulated signals, respectively.

In every case, the support for the foetal QRS complex was considered equal to 40 ms, centered around the R peak. Taking into account that the measurement on the QRS complex is limited to its peak-to-peak-amplitude, the chosen size allowed including only the relevant parts of the complex, according to the literature [58]. Moreover, the adoption of a larger time frame would not change the results unless for the possible inclusion of noise spikes.

Since the denoising should in principle help a foetal QRS detection algorithm, another performance index considered in this work was the accuracy and the true positive rate of a state-of-the-art peak detector [59], computed as:

$$Acc = TP/(TP + FP + FN) \quad (8)$$

$$TPR = TP/(TP + FN) \quad (9)$$

where *TP* is the number of true positives, *FP* is the number of false positives and *FN* is the number of false negatives.

All these performance indexes are important on real recordings because the actual fECG waveform morphology is unknown and it is impossible to assess the distortion introduced by the different post-processing methods. Conversely, this is possible on the simulated signals. To this aim, the RMSE, ρ and r_s were evaluated between each WD-processed simulated signal and the corresponding noiseless fECG signal. For each signal, considering an interval of 300 ms around each foetal R wave, 120 ms before and 180 ms after [58], the three indexes were computed for each beat and their median values were used as measures of signal morphology preservation.

2.4.2. WD approaches comparison and statistical analysis methodology

In order to reduce the number of comparisons, we preliminarily performed an assessment to identify the best adaptation of the Han *et al.* threshold to SWPT to be used for the subsequent analyses. To this aim, we compared all the available performance indexes computed on both datasets for each tested decomposition level. Then, we selected the best adaptation Han *et al.* threshold to SWPT for the subsequent analyses.

At this point, we could consider three thresholds (Minimax, Universal and Han *et al.*) for each of the two WD methods (SWT and SWPT). On them, a statistical analysis was performed to investigate the following aspects:

(i) *WD effectiveness* in terms of SNR, Acc and TPR. The comparisons were performed by considering denoised signals vs. raw signals, on both datasets, separately for six and seven decomposition levels;

(ii) *superiority of SWT or SWPT* in terms of SNR, Acc and TPR for both datasets and ρ, r_s and RMSE for the synthetic one only, for each decomposition level and threshold;

(iii) *the best decomposition level* for a given method, i.e., by considering the comparison among SWPT or SWT approaches grouped by decomposition level. The analysis was performed on the same metrics as in (ii);

(iv) *the best WD approach* for each of the two decomposition levels by comparing the performance of a given method (SWT and SWPT) and threshold against all the other approaches available at that decomposition level. The analysis was performed on the same metrics as in (ii).

The schematic representation of the comparative assessments discussed above is depicted in Fig. 4.

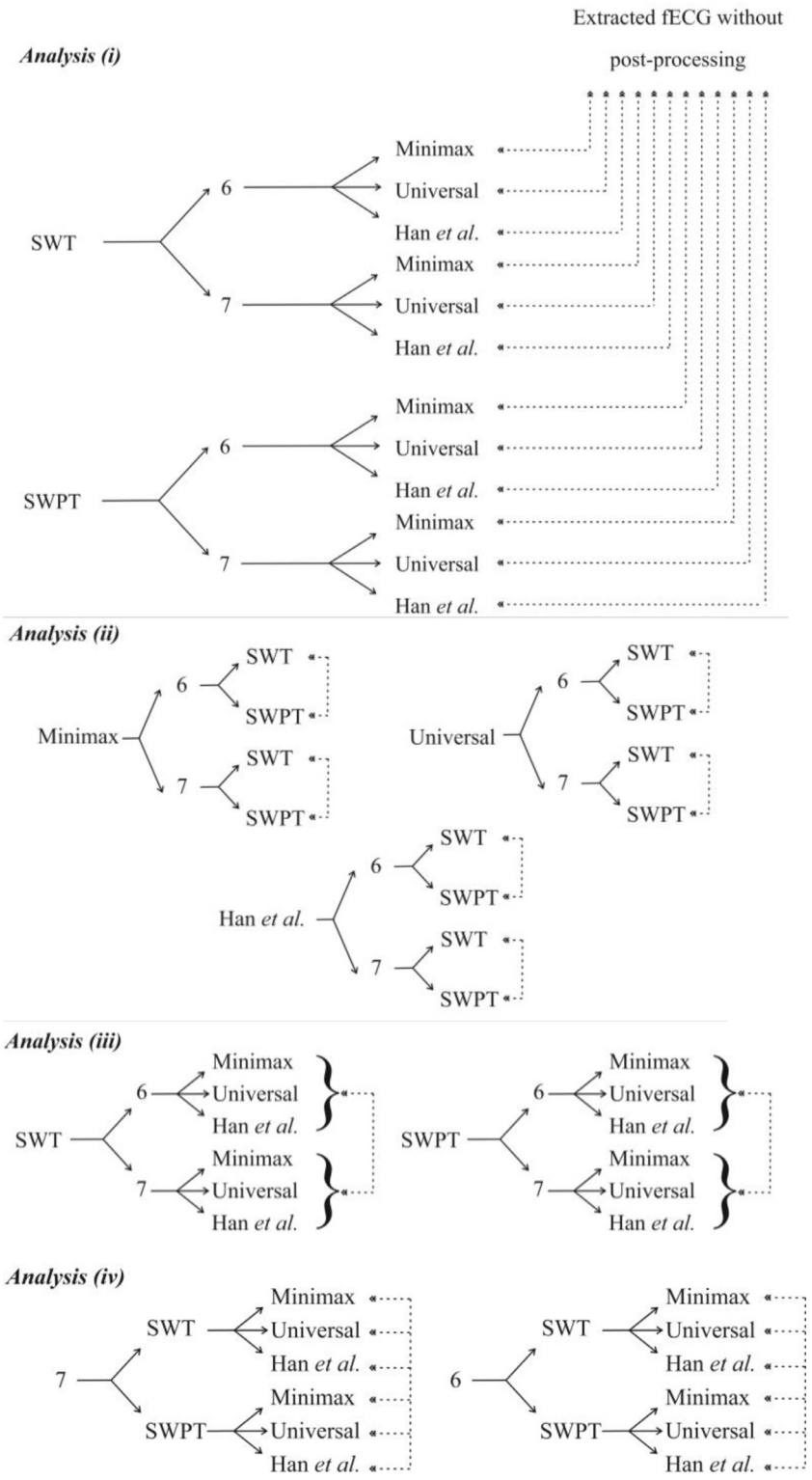

Fig. 4. General scheme of all the comparative analyses performed in this work. Dashed arrows represent the different comparisons carried out whereas solid arrows the wavelet parametrizations involved in each analysis. Two wavelet transforms (SWT and SWPT), along with the chosen levels of decomposition (6 and 7) and three thresholds (Minimax, Universal, Han *et al.*) were included in the comparative analyses. For the Han *et al.* threshold, the best SWPT adaptation identified in this work is reported.

For the statistical analysis, the normality of the distributions was preliminarily investigated by using the Lilliefors test. If a result did not satisfy the assumption of a normal distribution, a non-parametric statistical test was adopted. In specific, we used the Kruskal–Wallis test when comparing more than two distributions whereas the Wilcoxon test when comparing two distributions only. When the results of the Lilliefors test did not reject the assumption of a non-normal distribution, we adopted the one-way ANOVA instead of the Kruskal–Wallis test and the Student's t-test instead of the Wilcoxon test. Bonferroni correction was applied only when the goal of the analysis was the identification of the best solution, i.e. for the analysis (iv).

In all the statistical tests, we considered $p < 0.05$ for statistical significance.

All data processing was performed in MATLAB v2018b (MathWorks Inc., MA, USA).

3. Results

3.1. Best adaptation of the Han et al. threshold to SWPT

The analysis aiming at identifying the best adaptation of the Han *et al.* threshold to SWPT did not reveal any statistically significant difference among the three proposed approaches on both datasets. However, all methods improved the quality of the signals in terms of SNR ($p<0.05$ for the real dataset, $p<10^{-4}$ for the synthetic one) and TPR for real signals ($p<0.0004$) compared to the raw noisy signal, as can be seen in Fig. 5, but not in terms of accuracy in the QRS detection (data not shown).

Despite the non-significant statistical difference, the SWPT-LI was selected for the subsequent analyses because it is simpler than SWPT-CI and exhibits better performance than SWPT-SA in terms of SNR on real signals.

3.2. WD effectiveness

As can be seen in Fig. 6, the behavior of WD algorithms with their various parameterizations was different for the synthetic and real dataset. On the former, the SNR was always significantly improved ($p<10^{-4}$ and $p<0.0004$, respectively for six and seven decomposition levels) whereas on the latter only the Han *et al.* threshold produced a significant improvement in terms of SNR ($p<0.01$) with all the parameterizations. However, Minimax produced a significant SNR enhancement only with SWT ($p<0.004$) whereas Universal generally produced a significant reduction of the SNR ($p<0.04$, for all but the SWT with seven decomposition levels).

Focusing on the accuracy in the QRS detection, although with 6-level decompositions the median values of Acc for all the approaches exceeded those achievable on the noisy raw signals, no statistical significance was reached except for the SWT with Minimax on synthetic signals ($p = 0.04$). Moreover, with 7-level decompositions, WD significantly degraded the Acc with SWPT Universal and Minimax ($p<0.04$), on the synthetic dataset, and with all the methods ($p<0.02$) but the SWT Han *et al.* on the real one.

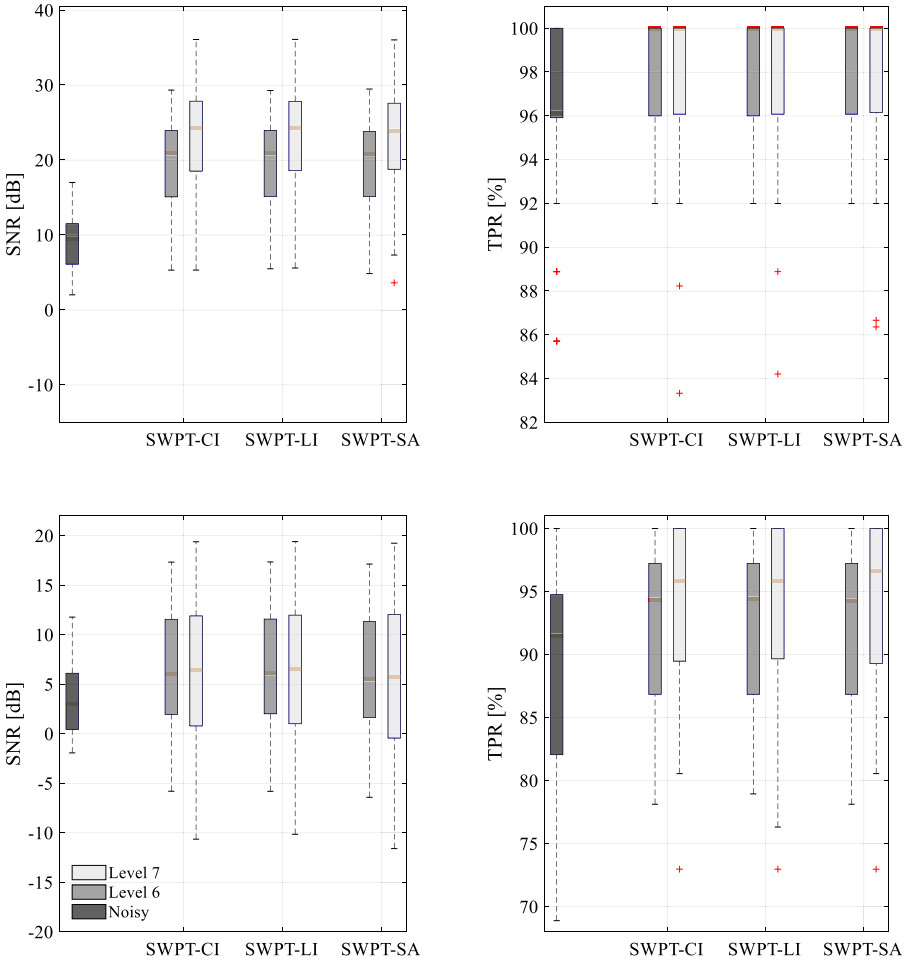

Fig. 5. SNR and TPR performance indexes for SWPT-CI, SWPT-LI and SWPT-SA denoised fECG signals with 6-level or 7-level decompositions and for raw noisy fECG signals. Top: results on the synthetic dataset. Bottom: results on the real dataset.

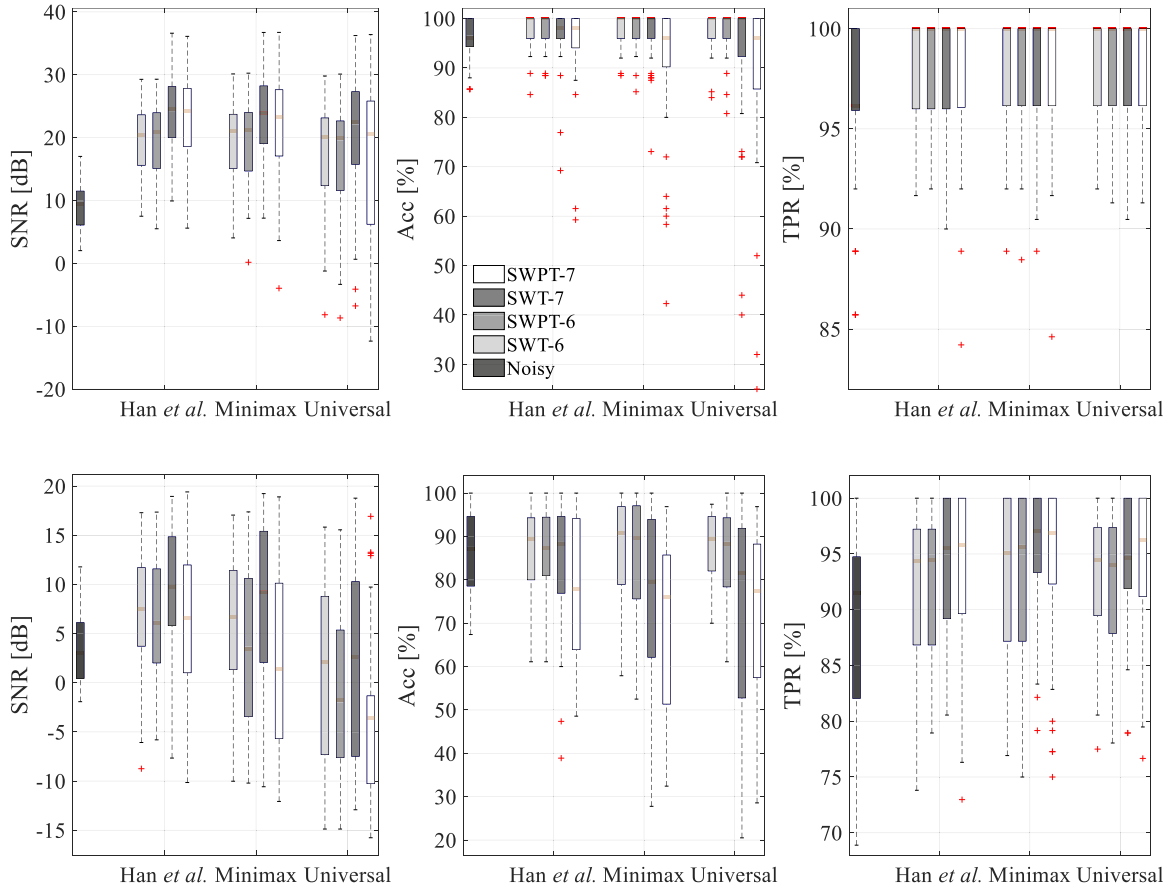

Fig. 6. WD effectiveness in terms of SNR, Accuracy and TPR on the synthetic dataset (top) and the real one (bottom).

Differently, TPR analysis showed that WD generally improved the QRS detector sensitivity with respect to the raw signals. On the real dataset, this was significant for all the algorithms (p<0.001), whereas on the synthetic dataset statistical significance was achieved only by Minimax (p<0.03 for both levels, SWT and SWPT) and Universal (p = 0.02, with 7-level SWT, and p = 0.03, with 6-level SWPT).

3.3. Superiority of SWT or SWPT

By exploiting the synthetic dataset, the results of this assessment in terms of the morphology preservation quality indexes are presented in Fig. 7. Even though the results appear to be quite similar, the statistical analysis revealed significantly better morphology preservation by SWT with respect to SWPT in terms of ρ, RMSE and r_s (p<0.04 for all thresholds and levels, except for the RMSE with Minimax at level six where no statistically significant difference was observed).

Moreover, by considering the performance indexes reported in Fig. 6, SWT was always superior in terms of SNR (p<0.0008) on real signals, whereas on the synthetic ones this superiority was statistically significant (p<0.0003) for Universal (both levels) and for Han *et al.* and Minimax (only for level seven). The same holds also for the Acc in all 7-level approaches on real signals, with a

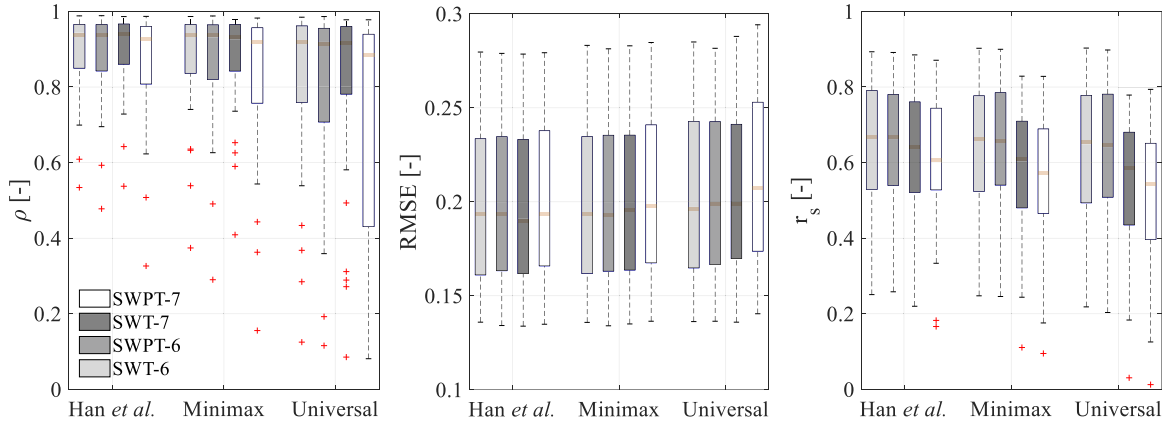

Fig. 7. Results obtained with the three selected thresholds on the simulated dataset for both decomposition levels (six and seven) and WD methods (SWT and SWPT) in terms of morphology preservation. Specifically: Pearson's correlation coefficient (ρ), RMSE and Spearman's rank correlation coefficient (r_s) distributions are reported in the different analysed cases.

noteworthy improvement with Minimax ($p = 0.004$) and Han *et al.* ($p = 0.0009$), and on synthetic signals for Minimax ($p = 0.0003$, level seven). No statistical difference was found in terms of TPR.

3.4. Best decomposition level

Fig. 8 shows that six decomposition levels allowed reaching significantly higher r_s values on both SWT and SWPT ($p<0.01$) on the synthetic signals. No other morphological performance indexes were revealing a statistically significant difference between the two methods.

By looking at the other indexes, six decomposition levels were significantly better in terms of Acc for the SWPT only ($p = 0.003$) on the synthetic dataset and for SWT and SWPT on the real one ($p = 0.0006$ and $p<10^{-4}$, respectively). Conversely, seven decomposition levels revealed significantly better results in terms of SNR for both SWT and SWPT ($p<0.02$) on the synthetic dataset and only for SWT on the real one ($p<0.05$). TPR followed a similar trend only on the real dataset ($p = 0.04$ and $p = 0.03$ for SWT and SWPT respectively).

3.5. Best WD approach

For the last analysis, we compared every parameterization with all the others, by keeping separate the different levels. On the synthetic dataset, the SWT with Han *et al.* threshold stood out as the best choice in 7-level decomposition in terms of Pearson's correlation coefficient only ($p<10^{-4}$ for all possible paired comparisons). On the real dataset, again SWT with Han *et al.* threshold outperformed all the other methods, this time in terms of SNR enhancement ($p<0.003$) with both levels (Figs. 6 and 7).

4. Discussion

The adoption of translation-invariant wavelet decomposition for noise reduction was already proven to be effective in fECG morphology preservation, both using complex wavelets [21] and comparing the same processing with the decimated WT [24]. However, focusing the attention on real WT only, no quantitative comparison can be found in the scientific literature for the fECG problem, since in [24] only simulated signals with unspecified characteristics and extracted by an adaptive neuro-fuzzy interference system (ANFIS) have been exploited.

Moreover, even though the SWPT was identified as a tool for powerline interference suppression on simulated fECG signals, albeit in an unconventional denoising approach [48], no previous works focused on its use on wide-band noise removal in fECG signals. Therefore, to the best of our knowledge, this work assessed in detail for the first time this kind of wavelet decomposition for fECG post-processing. Since one of the selected thresholds, the Han *et al.* one, was conceived for DWT and not for SWPT, we proposed

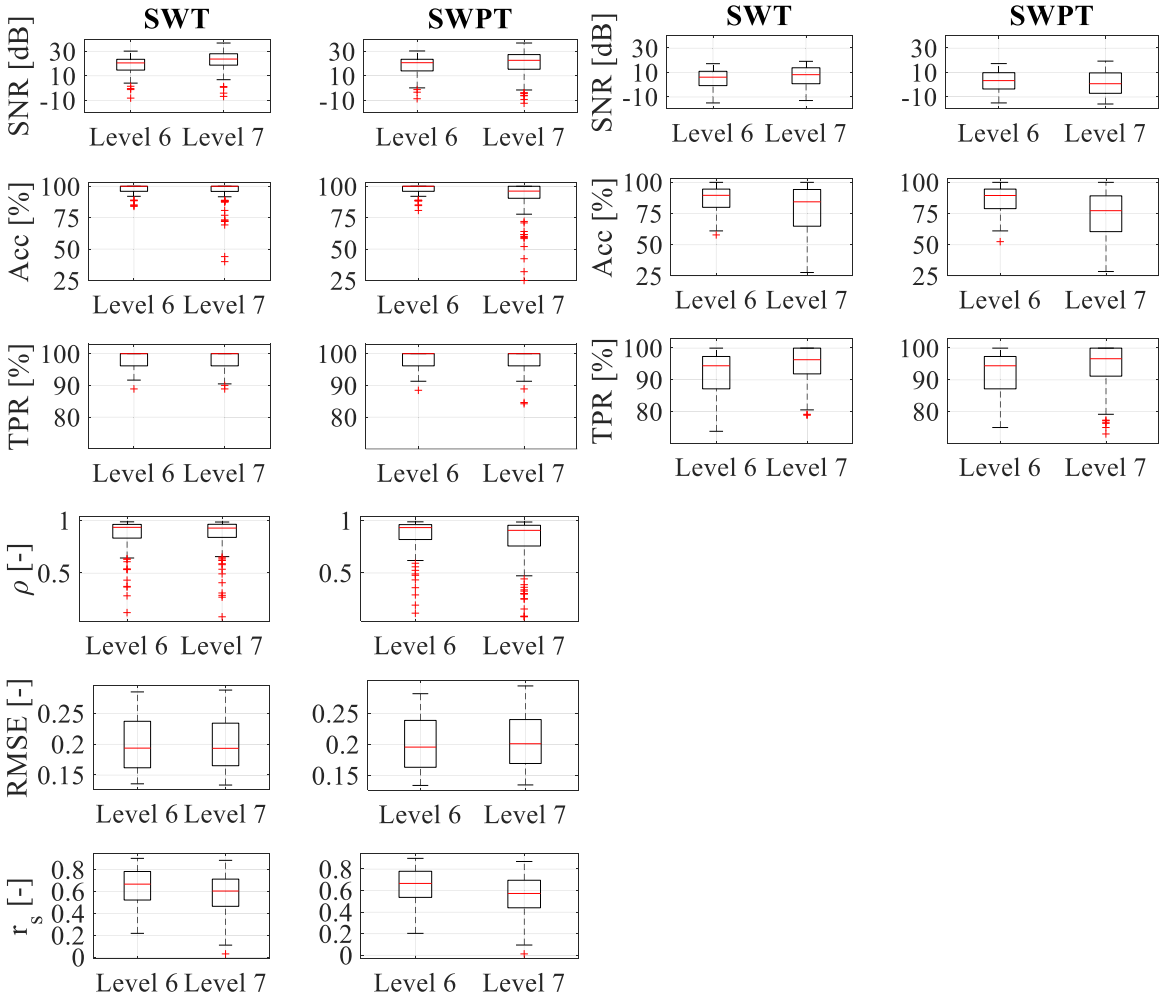

Fig. 8. Results obtained on the simulated dataset (first two columns, on the left) and on the real one (last two columns, on the right) for 6-level (Level 6) and 7-level (Level 7) decompositions, grouping all approaches by SWT and SWPT. The considerable number of outliers is due to the heterogeneity of the grouped distributions.

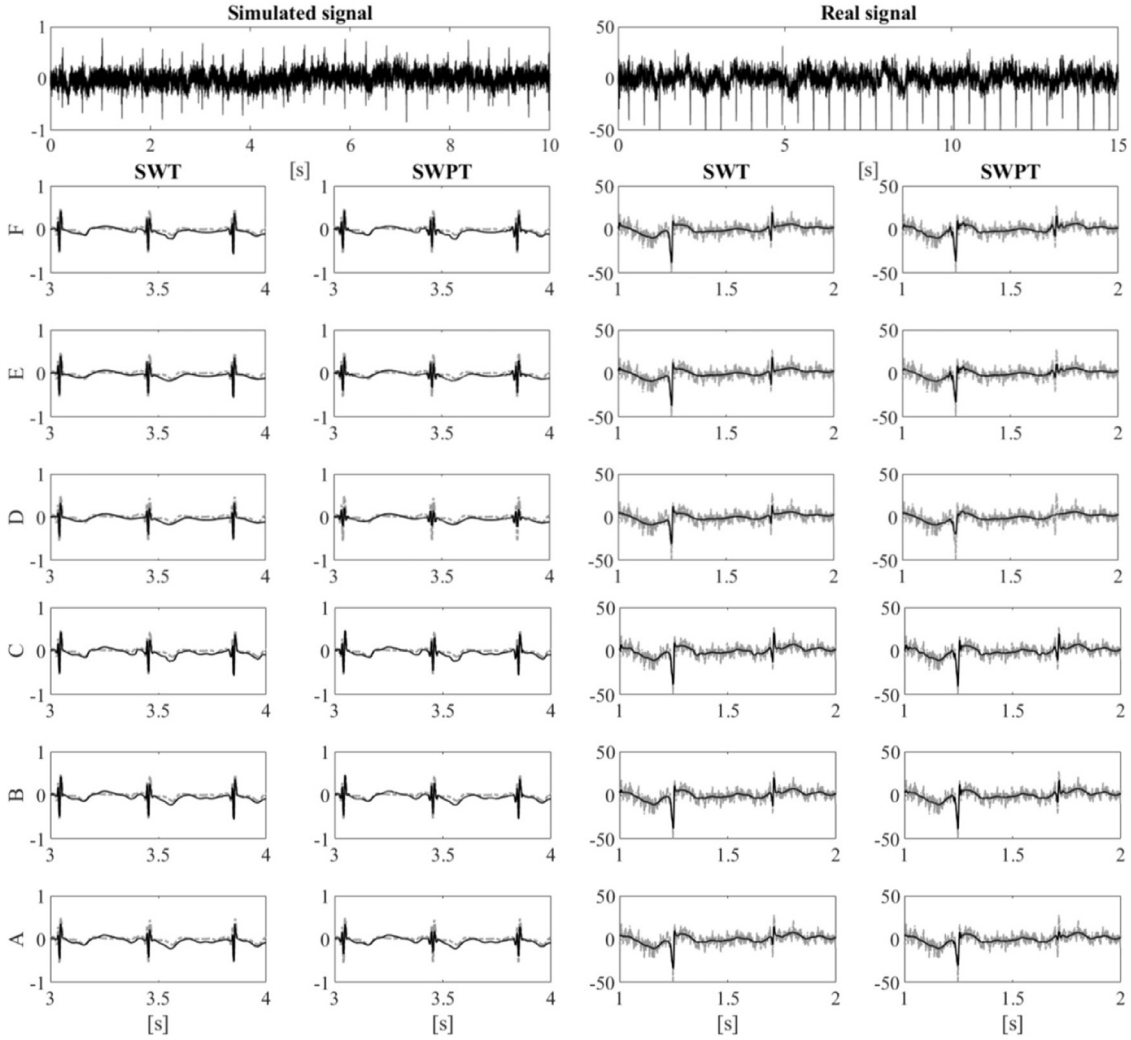

Fig. 9. Example of SWT and SWPT denoising results with both levels and decompositions with Universal (A, D for level six and seven respectively), Minimax (B, E for level six and seven respectively) and Han *et al.* threshold (C, F for levels six and seven, respectively). On the right, results obtained on a real extracted fECG signal from an abdominal recording were reported in μV; on the left, results obtained on a synthetic signal were represented. Zoom on one-second of each denoised fECG signal is reported to appreciate foetal beats morphology after wavelet denoising, with the original foetal beats in case of synthetic data and with the noisy traces in case of real ones (in gray).

and evaluated three different adaptations to the SWPT, which revealed a substantial equivalence from a statistical perspective.

Our findings confirmed the importance of WD as fECG post-processing tool. This result is in line with previous works, although in those cases WD was performed in different ways and after different fECG extraction algorithms [18,22,25,28]. Moreover, the datasets that have been exploited in the related works, both real and synthetic, [17,18,29–31,19,20,22,23,25–28] were heterogeneous, so that a quantitative comparison with our results was not possible. Moreover, a quantitative analysis of the post-processing results is frequently missing in the related works [22,25,29,30] or a complete definition of the selected implementation choices is not clearly stated [17,19,20,22,23,27]. Nevertheless, in [18] the effectiveness of WD as a post-processing tool for fECG signals was claimed, revealing how this technique could offer better performance in terms of fECG enhancement than its use as pre-processing or as both pre- and post-processing steps. However, the extraction process was carried out by a polynomial network and quantitative analysis was performed only on synthetic data in terms of SNR, whose improvement cannot be clearly quantified. A similar assessment was proposed in [28], where ANFIS was adopted as a separation algorithm. However, in this case, the adoption of WD is totally different from the typical use, retaining only the approximation coefficients and thus producing only a low-pass filtering behavior. WD introduced an SNR improvement also in [19], where the extraction of foetal components was not performed due to the different recording system, and in [5], in which the WD noise removal was assessed on a single simulated trace affected by muscular or powerline interference.

In the light of this scenario, our findings quantitatively revealed the performance of WD as fECG post-processing tool and, thanks to the open data availability [36], can provide a benchmark for other fECG post-processing algorithms. Moreover, our results can be generalised to different fECG recordings and projections, since our real dataset included different foetal heartbeat morphologies (see Fig. 7 in [36]).

From our results, it was clear that WD was generally unsuccessful in improving the accuracy of the foetal QRS detection, at least with the foetal QRS detector chosen in this work [59]. In fact, by focusing at first on the real signals, WD algorithms generally improved the accuracy of the foetal detection with 6-level decompositions, but not significantly, probably because of the high accuracy values already achieved on the raw signals. On the other hand, forcing the denoising effect until 8 Hz (i.e. with 7-level decompositions), the accuracy performance was generally worse except for Han *et al.* threshold in SWT implementations. Neverthe-

less, the TPR analysis revealed that WD significantly enhanced the sensitivity of the foetal QRS detector on both datasets. By looking at (8) and (9), we can relate the accuracy and TPR behaviors to the increase in FP number when using WD, probably due to the aggressive denoising that emphasized the residual artefacts compared with the background noise, challenging the QRS detector.

Despite the results obtained on the QRS detection, the SNR was generally improved by WD, as expected [18]. On the synthetic signals, this finding was statistically demonstrated for all the methods, thresholds and levels, whereas SNR results showed less homogeneity on the real signals. Excluding Han *et al.* threshold, which presented a significantly higher SNR regardless of the WD method and the decomposition level, Minimax achieved significant improvement only when used in combination with the SWT. On the other hand, Universal generally failed in improving the SNR of the signal. This evidence is consistent with [27,31], where the superiority of Minimax with respect to Universal was proven considering hard thresholding, despite their quantitative analyses were carried out only on simulated data. However, this difference in SNR performance among thresholds is probably due to the shrinkage effect due to the threshold amplitudes. In fact, the Universal threshold presented the higher scaling factor of σ_j with respect to the other thresholds, whereas Han *et al.* threshold achieved higher values than Minimax up to level 3, i.e. at higher frequencies, being more conservative below 128 Hz.

As regards the WD methods, SWT-based approaches outperform the more complex SWPT-based ones in fECG post-processing. Our analysis showed that SNR and the QRS detection accuracy were significantly higher in the SWT-based algorithms with respect to SWPT-based ones, despite these findings were not always statistically significant. Moreover, on synthetic signals, the SWT methods demonstrated a significantly superior capability to preserve the fECG signal morphology. Overall, the SWT outperformed the SWPT, and the adoption of seven levels for the decomposition of the signal provided more relevant improvement in the performance of the former method compared with the latter.

By comparing all possible WD methods involved in this work, the Han *et al.* threshold with SWT decomposition significantly outperformed all the other approaches in terms of ρ (on the synthetic dataset) and SNR (on the real dataset), despite statistical significance was rarely achieved. This result further confirmed the superiority of the SWT over the SWPT.

Finally, by focusing on the level of decomposition, 6-level decomposition preserved the most the morphology of the underlying fECG signal, because the Spearman's rank correlation (on the synthetic dataset) and the accuracy (on both datasets) were significantly higher at this level for all the WD methods. These findings suggested a less aggressive denoising with six levels of decomposition with respect to seven levels, as confirmed by the higher SNR values of the latter on both datasets, at least for the SWT. This result is coherent with the fact that 7-level decompositions introduce thresholding in a part of the signal band that is preserved in the 6-level case.

However, Fig. 9 visually shows how the SWT reached a better performance in terms of waveform distortion than the SWPT (which in turn reduces the amplitude of the foetal R peaks). Fig. 9 also suggests that, regardless the chosen WD method, the different thresholds can produce substantial differences in the morphology of the fECG trace, particularly emphasized by the Universal threshold that often leads to complete cancellation of the foetal beats. Qualitative and quantitative analyses confirmed that the Han *et al.* threshold with SWT is the best approach for the denoising of fECG signals after signal separation, even though the Minimax threshold also achieved good denoising performance.

Finally, even though WD is typically suitable for real-time processing, some points must be analysed. Remarkably, after setting the signal length and the level of decomposition to be exploited, the computational complexity associated to the three thresholds compared in this work can be considered equal, since all the scaling factors can be pre-computed off-line. Nonetheless, in this context, the computational complexity of the fECG post-processing is not considerably affected by the chosen WD algorithm but rather by the other algorithms involved in the evaluation of the σ_j, i.e. the fECG extraction method, the maternal ECG delineator and the foetal QRS detector, whose computational load depends on the selected algorithms and its estimation is beyond the scope of this study.

5. Conclusions

The quality improvement of the fECG signals obtained from non-invasive biopotential recordings is a key aspect for the adoption of this technique in the clinical practice. Despite the widespread application of WD on different biomedical signals, this powerful tool must be used with special care in this particular application because of its possible negative impact on the signal morphology or even on further signal processing steps applied downstream, such as the foetal QRS detection.

The results of the present study reveal how the adoption of a level-dependent scaling factor in the definition of the threshold significantly improves the denoising effectiveness compared with conventional approaches such as Minimax and Universal. SWT is generally preferable to the SWPT not only in terms of noise reduction (SNR) but also in terms of signal morphology preservation. Moreover, the finer decomposition of the lower frequency band obtained by increasing the number of decomposition levels, even though producing a better result in terms of noise reduction, is responsible for a morphological degradation of the signal.

All these aspects could be valuably considered when approaching the denoising of fECG signals for quality improvement, thus contributing to the exploitation of this important signal for antenatal cardiological assessment.

Declaration of Competing Interest

The authors have no conflicts of interest to disclose.

Acknowledgments

The authors wish to thank the team headed by Dr. Roberto Tumbarello, Division of Paediatric Cardiology, S. Michele Hospital (Cagliari, Italy), for the important support, and Elisa Brungiu for her support in the preliminary signal processing investigation. We also wish to acknowledge all the involved voluntary pregnant women. Eleonora Sulas is grateful to Sardinia Regional Government for supporting her PhD scholarship (P.O.R. F.S.E., European Social Fund 2014–2020). Part of this research was supported by the Italian Government—Progetti di Interesse Nazionale (PRIN) under the grant agreement 2017RR5EW3 - ICT4MOMs project.

Supplementary materials

Supplementary material associated with this article can be found, in the online version, at doi:10.1016/j.cmpb.2020.105558.

References

[1] M.T. Donofrio, A.J. Moon-Grady, L.K. Hornberger, J.A. Copel, M.S. Sklansky, A. Abuhamad, B.F. Cuneo, J.C. Huhta, R.A. Jonas, A. Krishnan, S. Lacey, W. Lee, E.C. Michelfelder, G.R. Rempel, N.H. Silverman, T.L. Spray, J.F. Strasburger, W. Tworetzky, J. Rychik, Diagnosis and treatment of fetal cardiac disease, Circulation 129 (2014) 2183–2242 https://doi.org/10.1161/01.cir.0000437597.44550.5d.

[2] R. Weber, D. Stambach, E. Jaeggi, Diagnosis and management of common fetal arrhythmias, J. Saudi Hear. Assoc. 23 (2011) 61–66 https://doi.org/10.1016/j.jsha.2011.01.008.

[3] T.F. Oostendorp, A. van Oosterom, H.W. Jongsma, Electrical properties of tissues involved in the conduction of foetal ECG, Med. Biol. Eng. Comput. 27 (1989) 322–324.

[4] R. Sameni, G.D. Clifford, A Review of Fetal ECG Signal Processing; Issues and Promising Directions, Open Pacing. Electrophysiol. Ther. J. 3 (2010) 4–20 https://doi.org/10.2174/1876536X01003010004.

[5] R. Martinek, R. Kahankova, J. Nedoma, M. Fajkus, K. Cholevová, Fetal ECG Preprocessing Using Wavelet Transform, in: Proceedings of the 10th International Conference on Computer Modeling and Simulation, 2018, pp. 39–43. https://doi.org/10.1145/3177457.3177503.

[6] R. Kahankova, R. Martinek, R. Jaros, K. Behbehani, A. Matonia, M. Jezewski, J.A. Behar, A review of signal processing techniques for non-invasive fetal electrocardiography, IEEE Rev. Biomed. Eng. (2019).

[7] A. Khamene, S. Negahdaripour, A new method for the extraction of fetal ECG from the composite abdominal signal, IEEE Trans. Biomed. Eng. 47 (2000) 507–516 https://doi.org/10.1109/10.828150.

[8] S. Almagro, M.M. Elena, M.J. Bastiaans, J.M. Quero, A new mother wavelet for fetal electrocardiography, to achieve optimal denoising and compressing results, in: 2006 Comput. Cardiol., 2006, pp. 157–160.

[9] H. Hassanpour, A. Parsaei, Fetal ECG Extraction Using Wavelet Transform, in: 2006 Int. Conf. Comput. Intel. Model. Control Autom. Int. Conf. Intell. Agents Web Technol. Int. Commer., 2006, p. 179. https://doi.org/10.1109/CIMCA.2006.98.

[10] R. Almeida, H. Goncalves, J. Bernardes, A.P. Rocha, Fetal QRS detection and heart rate estimation: a wavelet-based approach, Physiol. Meas. 35 (2014) 1723–1735 https://doi.org/10.1088/0967-3334/35/8/1723.

[11] S. Ziani, A. Jbari, L. Belarbi, Fetal electrocardiogram characterization by using only the continuous wavelet transform CWT, in: 2017 Int. Conf. Electr. Inf. Technol., 2017, pp. 1–6. https://doi.org/10.1109/EITech.2017.8255310.

[12] M.G. Jafari, J.A. Chambers, Fetal electrocardiogram extraction by sequential source separation in the wavelet domain, IEEE Trans. Biomed. Eng. 52 (2005) 390–400 https://doi.org/10.1109/TBME.2004.842958.

[13] G. Liu, Y. Luan, An adaptive integrated algorithm for noninvasive fetal ECG separation and noise reduction based on ICA-EEMD-WS, Med. Biol. Eng. Comput. 53 (2015) 1113–1127 https://doi.org/10.1007/s11517-015-1389-1.

[14] S.L. Lima-Herrera, C. Alvarado-Serrano, P.R. Hernández-Rodríguez, Fetal ECG extraction based on adaptive filters and Wavelet Transform: validation and application in fetal heart rate variability analysis, in: 2016 13th Int. Conf. Electr. Eng. Comput. Sci. Autom. Control, 2016, pp. 1–6. https://doi.org/10.1109/ICEEE.2016.7751243.

[15] S. Wu, Y. Shen, Z. Zhou, L. Lin, Y. Zeng, X. Gao, Research of fetal ECG extraction using wavelet analysis and adaptive filtering, Comput. Biol. Med. 43 (2013) 1622–1627 https://doi.org/10.1016/j.compbiomed.2013.07.028.

[16] M. Suganthy, S. Manjula, Enhancement of SNR in fetal ECG signal extraction using combined SWT and WLSR in parallel EKF, Cluster Comput 22 (2019) 3875–3881 https://doi.org/10.1007/s10586-018-2477-4.

[17] M. Ma, N. Wang, S.-Y. Lei, Extraction of FECG based on time frequency blind source separation and wavelet de-noising, in: 2009 3rd Int. Conf. Bioinforma. Biomed. Eng., IEEE, 2009, pp. 1–3.

[18] M. Ahmadi, M. Ayat, K. Assaleh, H. Al-Nashash, Fetal ECG signal enhancement using polynomial classifiers and wavelet denoising, in: 2008 Cairo Int. Biomed. Eng. Conf., 2008, pp. 1–4. https://doi.org/10.1109/CIBEC.2008.4786095.

[19] F.N. Jamaluddin, Z.A.K. Bakti, M. Kamal, A. Aminudin, Wavelet analysis on FECG detection using two electrodes system device, Int. J. Integr. Eng. (2013) 5.

[20] V. Ionescu, Fetal ECG extraction from multichannel abdominal ECG recordings for health monitoring during labor, Procedia Technol 22 (2016) 682–689.

[21] Y. Ishikawa, H. Horigome, A. Kandori, H. Toda, Z. Zhang, Noise reduction by perfect-translation-invariant complex discrete wavelet transforms for fetal electrocardiography and magnetocardiography, Int. J. Wavelets, Multiresolution Inf. Process. 12 (2014) 1460008.

[22] N. Ivanushkina, K. Ivanko, E. Lysenko, I. Borovskiy, O. Panasiuk, Fetal electrocardiogram extraction from maternal abdominal signals, 2014 IEEE 34th Int. Sci. Conf. Electron. Nanotechnol., IEEE, 2014 334–338.

[23] M.S.H. Jadhav, M.D.N. Dhang, Extraction of Fetal ECG from Abdominal Recordings Combining BSS-ICA & WT Techniques, Int. J. Eng. Res. Technol. (2017) 10.

[24] S.H. Jothi, K.H. Prabha, Fetal electrocardiogram extraction using adaptive neuro-fuzzy inference systems and undecimated wavelet transform, IETE J. Res. 58 (2012) 469–475.

[25] F. Mochimaru, Y. Fujimoto, Y. Ishikawa, The fetal electrocardiogram by independent component analysis and wavelets, Jpn. J. Physiol. 54 (2004) 457–463.

[26] B. Rivet, V. Vigneron, A. Paraschiv-Ionescu, C. Jutten, Wavelet de-noising for blind source separation in noisy mixtures, in: Int. Conf. Indep. Compon. Anal. Signal Sep., Springer, 2004, pp. 263–270.

[27] Mohammad Shayesteh, Jamal Falahian, Using Wavelet Transformation in Blind Sources Separation of the Fetal Electrocardiogram, Majlesi Journal of Electrical Engineering (2011) 185–193.

[28] Rajaguru Swarnalatha, D.V. Prasad, Maternal ECG cancellation in abdominal signal using ANFIS and wavelets, Journal of Applied Sciences 10 (2010) 868–877, doi:10.3923/jas.2010.868.877.

[29] V. Vigneron, A. Paraschiv-Ionescu, A. Azancot, O. Sibony, C. Jutten, Fetal electrocardiogram extraction based on non-stationary ICA and wavelet denoising, in: Seventh Int. Symp. Signal Process. Its Appl. 2003. Proceedings, IEEE, 2003, pp. 69–72.

[30] Y. Wang, Y. Fu, Z. He, Fetal Electrocardiogram Extraction Based on Fast ICA and Wavelet Denoising, in: 2018 2nd IEEE Adv. Inf. Manag. Autom. Control Conf., 2018, pp. 466–469. https://doi.org/10.1109/IMCEC.2018.8469501.

[31] E. Castillo, D.P. Morales, A. García, F. Martínez-Martí, L. Parrilla, A.J. Palma, Noise suppression in ECG signals through efficient one-step wavelet processing techniques, J. Appl. Math. (2013) 2013.

[32] G. Baldazzi, E. Sulas, E. Brungiu, M. Urru, R. Tumbarello, L. Raffo, D. Pani, Wavelet-Based Post-Processing Methods for the Enhancement of Non-Invasive Fetal ECG, Comput. Cardiol. 46 (2019) 2019 https://doi.org/10.22489/CinC.2019.345 .

[33] D.L. Donoho, J.M. Johnstone, Ideal spatial adaptation by wavelet shrinkage, Biometrika 81 (1994) 425–455.

[34] D.L. Donoho, De-noising by soft-thresholding, IEEE Trans. Inf. Theory. 41 (1995) 613–627.

[35] M. Han, Y. Liu, J. Xi, W. Guo, Noise Smoothing for Nonlinear Time Series Using Wavelet Soft Threshold, Signal Process. Lett. IEEE 14 (2007) 62–65 https://doi.org/10.1109/LSP.2006.881518.

[36] G. Baldazzi, E. Sulas, M. Urru, R. Tumbarello, L. Raffo, D. Pani, Annotated real and synthetic datasets for non-invasive foetal electrocardiography post-processing benchmarking, Data Br. (n.d.).

[37] M. Misiti, Y. Misiti, G. Oppenheim, J.-.M. Poggi, Wavelets and their Applications, Wiley Online Library, 2007.

[38] S. Mallat, A Wavelet Tour of Signal Processing, Elsevier, 1999.

[39] M. Unser, A. Aldroubi, A review of wavelets in biomedical applications, Proc. IEEE 84 (1996) 626–638.

[40] L. Sörnmo, P. Laguna, Bioelectrical Signal Processing in Cardiac and Neurological Applications, Academic Press, 2005.

[41] I.M. Johnstone, B.W. Silverman, Wavelet threshold estimators for data with correlated noise, J. R. Stat. Soc. Ser. B (Statistical Methodol. 59 (1997) 319–351.

[42] R.R. Coifman, D.L. Donoho, Translation-invariant de-noising, in: Wavelets Stat, Springer, 1995, pp. 125–150.

[43] G.P. Nason, B.W. Silverman, The stationary wavelet transform and some statistical applications, in: Wavelets Stat., Springer, 1995, pp. 281–299.

[44] J.-.C. Pesquet, H. Krim, H. Carfantan, Time-invariant orthonormal wavelet representations, IEEE Trans. Signal Process 44 (1996) 1964–1970.

[45] D.B. Percival, A.T. Walden, Wavelet Methods For Time Series Analysis, Cambridge university press, 2006.

[46] A.T. Walden, A. Contreras Cristan, The phase–corrected undecimated discrete wavelet packet transform and its application to interpreting the timing of events, Proc. R. Soc. Lond. A. 454 (1998) 2243–2266 https://doi.org/10.1098/rspa.1998.0257.

[47] G.D. Clifford, I. Silva, J. Behar, G.B. Moody, Non, -invasive fetal ECG analysis, Physiol. Meas 35 (2014) 1521.

[48] D.-.D. Ţarălungă, G.-.M. Ungureanu, I. Gussi, R. Strungaru, W. Wolf, Fetal ECG extraction from abdominal signals: a review on suppression of fundamental power line interference component and its harmonics, Comput. Math. Methods Med. 2014 (2014).

[49] J. Behar, F. Andreotti, S. Zaunseder, Q. Li, J. Oster, G.D. Clifford, An ECG simulator for generating maternal-foetal activity mixtures on abdominal ECG recordings, Physiol. Meas. 35 (2014) 1537 https://doi.org/10.1088/0967-3334/35/8/1537.

[50] F. Andreotti, J. Behar, S. Zaunseder, J. Oster, G.D. Clifford, An open-source framework for stress-testing non-invasive foetal ECG extraction algorithms, Physiol. Meas. 37 (2016) 627.

[51] A.L. Goldberger, L.A.N. Amaral, L. Glass, J.M. Hausdorff, P.C. Ivanov, R.G. Mark, J.E. Mietus, G.B. Moody, C.-.K. Peng, H.E. Stanley, PhysioBank, PhysioToolkit, and PhysioNet: components of a new research resource for complex physiologic signals, Circulation 101 (2000) e215–e220.

[52] R. Sameni, The Open-Source Electrophysiological Toolbox (OSET), version 3.14, (2018). https://www.researchgate.net/publication/235325036_The_Open-Source_Electrophysiological_Toolbox_OSET_version_21.

[53] J.A. Apolinario, JR, QRD-RLS Adaptive Filtering, Springer, 2009.

[54] E. Sulas, M. Urru, R. Tumbarello, L. Raffo, D. Pani, Systematic analysis of single- and multi-reference adaptive filters for no'n-invasive fetal electrocardiography, Math. Biosci. Eng. 17 (n.d.) 286–308. http://dx.doi.org/10.3934/mbe.2020016.

[55] E. Sulas, M. Urru, R. Tumbarello, L. Raffo, D. Pani, Comparison of Single and Multi-Reference QRD-RLS Adaptive Filter for Non-Invasive Fetal Electrocardiography, EMBC, 2019.

[56] S. Ravindrakumar, K. Bommannaraja, Certain Investigation On De-Noising The Multichannel Abdominal ECG Signal Using Various Adaptive Noise Suppression Techniques, Aust. J. Basic Appl. Sci. (2015) 372–380.

[57] J.P. Martinez, R. Almeida, S. Olmos, A.P. Rocha, P. Laguna, A wavelet-based ECG delineator: evaluation on standard databases, IEEE Trans. Biomed. Eng. 51 (2004) 570–581 https://doi.org/10.1109/TBME.2003.821031.

[58] M.J.O. Taylor, M.J. Smith, M. Thomas, A.R. Green, F. Cheng, S. Oseku-Afful, L.Y. Wee, N.M. Fisk, H.M. Gardiner, Non-invasive fetal electrocardiography in singleton and multiple pregnancies, BJOG 110 (2003) 668–678.

[59] J. Behar, J. Oster, G.D. Clifford, Combining and benchmarking methods of foetal {ECG} extraction without maternal or scalp electrode data, Physiol. Meas. 35 (2014) 1569–1589 https://doi.org/10.1088/0967-3334/35/8/1569.